

Entropy Production in Laser Heating of Silicon-Germanium Thin Films

J. Ernesto Nájera-Carpio

Instituto de Energías Renovables, UNAM
Privada de Xochicalco S/N, Temixco, Mor., México
najerarpio@gmail.com

Federico Vázquez

Universidad Autónoma del Estado de Morelos, Facultad de Ciencias
Av. Universidad 1001, Col. Chamilpa, Cuernavaca, Mor., México
vazquez@uaem.mx

Abstract - In the present study the entropy production in laser heating of Silicon-Germanium thin films is examined. The film consists of three layers in two possible arrays, namely, Si-Ge-Si and Ge-Si-Ge. Silicon and Germanium are subjected to the laser irradiation respectively. Total width of the array is 200 nm in all cases. The heat transport in the array is described by the energy conservation equation with a source term representing the absorption of laser radiation in the medium. The boundary condition for the temperature is of Dirichlet type. The three layer system is modelled by considering it a heterogeneous media where the heat conductivity coefficient depends on position. We present the stationary temperature and entropy production profiles together with the global entropy production in the system as a function of total Silicon length in the array. We calculate the stationary global entropy production by integrating the local production in the width of the film. Our main result concerns the existence of maxima and minima in the global entropy production. The Ge-Si-Ge array presents a remarkable maximum at a total length of Silicon of 145 nm. These results may be useful in designing of thin films used in electronic industry where the control of irreversible processes is important.

Keywords: Entropy production, Thin films, Silicon-Germanium arrays, Laser heating.

1. Introduction

The entropy production analysis is useful for the study of dissipation and irreversibility of different processes in physics and engineering of nanoscaled systems. The minimum entropy production principle states that the system evolves in time reaching a minimum entropy production rate at the stationary state. This establishes a relation between irreversible processes and optimal performance of the system. Thin films are widely used in electronic industry. Considerable research studies are being carried out to examine the energy transport in those systems and their optimal performance (Figueroa and Vázquez, 2014) and durability. The effects of laser heating of dielectric thin films have attracted particular interest in the scientific community (Yilbas and Al-Dweik, 2013; Mansoor and Yilbas, 2011; Lewandowska and Malinowski, 2006). In this work we address the problem of laser heating of Si-Ge thin films under the scope of irreversible processes produced during the heat transport in the system. We model an array of Si-Ge layers within the framework of thermodynamics of irreversible processes (Jou et al., 2001). In Section 2 we give a brief description of the studied system and the used methods to model heat transport and entropy production. Our results can be seen in Section 3. Finally, a discussion with some concluding remarks can be found in Section 4. Our main result is to show the existence of minimum entropy production states determined by specific material distribution in the system.

2. Methods

Due to the progress in the microscaling techniques the film thickness may reduce to become comparable to the phonon mean free path (PMFP). When the thickness is below the PMFP the heat transport regime becomes of the ballistic type. This may make necessary to use a radiative transport equation to describe energy transfer (Joshi and Majumdar, 1993). Otherwise, the transport pertains to the diffusive regime. Considering this, in this work the film thickness of the array is constrained to be above the PMFP in such a way that the classical Fourier equation represents a valid autonomous mesoscopic theory to describe heat transfer. We then combine Fourier equation with the internal energy conservation to get the transport equation where the incident laser energy is incorporated as a volumetric heat source to account for the absorption of energy by the medium. It is also included the effect of the layer thickness on the heat conductivity. The expression for it is obtained in the framework of extended irreversible thermodynamics. This allows us to describe the experimentally observed diminishing of the thermal conductivity when the layer thickness approaches the PMFP. The transport equation is solved with Dirichlet type boundary condition for the temperature.

2. 1. The System

The three layer system is schematically shown in Figure 1. The incidence of the Laser beam is always from the left as it can be seen. The thickness of the system is given by $L = L_1 + L_2 + L_3$. The boundary condition is $T(0) = T(L) = 300K$. Equal temperatures are assumed at the interfaces.

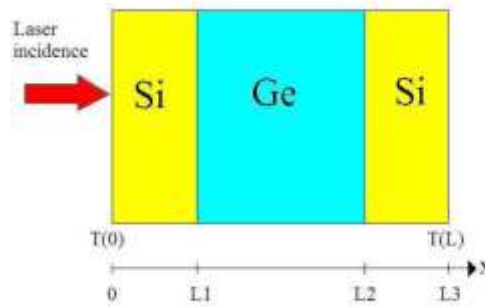


Fig. 1. A schematic view of a Si-Ge-Si array consisting of three layers of thickness L_1 , L_2 and L_3 .

$T(0) = T(L) = 300K$. The system Ge-Si-Ge can be represented by a similar scheme as the shown in this figure.

2. 2. Mathematical Model

The governing system of equations of heat transport can then be written as follows:

$$\rho_s C_v \frac{\partial T}{\partial t} = K(L) \frac{\partial^2 T}{\partial x^2} + P, \quad (1)$$

where ρ_s is the volumetric mass density, C_v the specific heat, $K(L)$ the thickness dependent heat conductivity, P the source term which represents the absorption of laser radiation in the medium. In the stationary state Eq. (1) reads as

$$K(L) \frac{\partial^2 T}{\partial x^2} + P = 0. \quad (2)$$

The expression for the source term depends on the position of the layer within the array. In the case that the layer is in the side of the incident laser it is given by

$$P = \frac{\eta_v}{2\mu_0 c L} E_0^2 T_{v1} (1 + e^{-\alpha L} (-1 + R_{12} (1 - e^{-\alpha L}))). \quad (3)$$

In this equation E_0 is the electric field amplitude of the incident laser, α the absorption coefficient of the medium, L the thickness and η_v and μ_0 the refraction index and the magnetic permeability of empty space, respectively. Two optical coefficients are included in Eq. (3):

$$T_{v1} = \frac{\eta_1}{\eta_v} \left(\frac{2\eta_v}{\eta_v + \eta_1} \right)^2, \quad (4)$$

$$R_{12} = \left(\frac{\eta_v - \eta_1}{\eta_v + \eta_1} \right)^2. \quad (5)$$

η_1 is the refraction index of the medium, T_{v1} is the transmission coefficient from the empty space to the medium and R_{12} is the reflection coefficient of the following layer.

Finally, we use two results obtained along with the irreversible thermodynamics principles, namely, the entropy production S (Jou et al., 2001) and the thickness dependent heat conductivity $K(L)$ (Álvarez and Jou, 2007). The first one is written as follows:

$$S = -\frac{J_q}{T^2} \frac{\partial T}{\partial x}, \quad (6)$$

where the heat flux is given by the classical Fourier equation

$$J_q = -K(L) \frac{\partial T}{\partial x}, \quad (7)$$

and the second one reads

$$K(L) = \frac{K_0 L^2}{2\pi^2 l^2} \left(\sqrt{1 + 4 \left(\frac{\pi l}{L} \right)^2} - 1 \right). \quad (8)$$

In Eq. (8) K_0 is the bulk heat conductivity, l the phonon mean free path in the medium and L the thickness of the layer.

3. Results

In this section our main results are displayed. They were obtained by using the following values for the involved parameters: $K_{0Si} = 148W / Km$, $K_{0Ge} = 59.9W / Km$, $l_{Si} = 7.6nm$, $l_{Ge} = 10.5nm$, $\eta_{Si} = \eta_{Ge} = 4.01$, $\alpha_{Si} = 1 \times 10^7 m^{-1}$, $\alpha_{Ge} = 7 \times 10^7 m^{-1}$, $E_0 = 6.14 \times 10^4 N / C$.

In Figure 2 we present the stationary temperature profile of $Si_{50}-Ge_{100}-Si_{50}$ (blue line) and $Ge_{50}-Si_{100}-Ge_{50}$ (red line) arrays when the lengths of the layers are 50 nm, 100 nm and 50 nm, respectively. In the notation used, the thickness of each layer is indicated by the subindex. This result was obtained by analytically solving Eq. (1) in the stationary state with Dirichlet type conditions $T(0) = T(L) = 300K$.

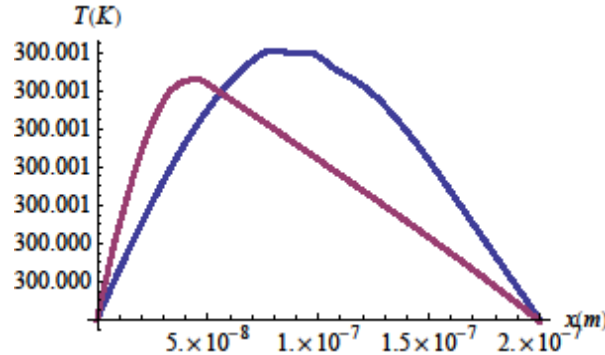


Fig. 2. Stationary temperature profiles for $Si_{50}-Ge_{100}-Si_{50}$ (blue) and $Ge_{50}-Si_{100}-Ge_{50}$ (red). The subindexes indicate the length (in nm) of the corresponding layer.

The stationary local entropy production in the profile can be seen in Figure 3 where the blue line corresponds to the $Si_{50}-Ge_{100}-Si_{50}$ array and the red one to $Ge_{50}-Si_{100}-Ge_{50}$. Note that the scale in the vertical axis is logarithmic.

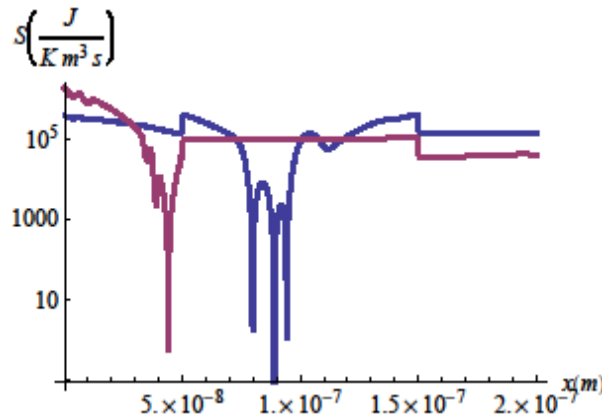


Fig. 3. Stationary entropy production profiles for $Si_{50}-Ge_{100}-Si_{50}$ (blue) and $Ge_{50}-Si_{100}-Ge_{50}$ (red). The subindexes indicate the length (in nm) of the corresponding layer.

Finally, in Figure 4 it can be seen the stationary global entropy production as a function of the total length of Silicon in the array. As above, the blue line corresponds to the $Si_{50}-Ge_{100}-Si_{50}$ array and the red one to $Ge_{50}-Si_{100}-Ge_{50}$. Each line was obtained by fitting a polynomial of degree 10 to the calculated discrete set of points. Note that the scale in the vertical axis is logarithmic. A discussion and concluding remarks are included in the following section.

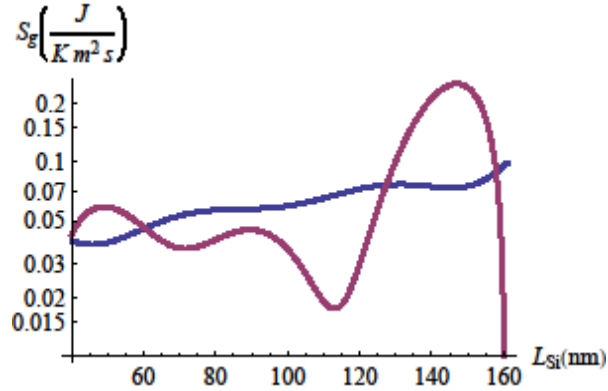


Fig. 4. Global entropy production vs. Total Silicon length L_1+L_3 (see Figure 1) for $\text{Si}_{50}\text{-Ge}_{100}\text{-Si}_{50}$ (blue) and L_2 for $\text{Ge}_{50}\text{-Si}_{100}\text{-Ge}_{50}$ (red). The subindexes indicate the length (in nm) of the corresponding layer.

4. Concluding Discussion

In this final section we make a brief discussion of our results and include some concluding remarks. First of all, it is necessary to mention that we have not considered the thermal interface resistance. For this reason the stationary temperature profiles are smooth curves. It must be noted that even when the material distribution of the system is symmetric the stationary temperature distribution in the profile is not symmetric. This is more marked in the case of the Ge-Si-Ge array due to the fact that the absorption coefficient of Germanium is bigger than that of Silicon. It must be also noted that the minima in the local entropy production shown in Figure 3 correspond to the maxima of the temperature profile (see Figure 2). Specifically, in the case of the Si-Ge-Si array the minimum in the local entropy production may be situated around $x=9\times 10^{-8}m$. In Figure 2, it can be observed that in such position there exists a maximum in the temperature. In the same manner, the minimum in the local entropy production of the Ge-Si-Ge array around $x=4\times 10^{-8}m$ corresponds to the maximum temperature at the same position. Note that in those positions the heat flux vanishes. Referring now to Figure 4 it is worth mentioning that when the Si-Ge-Si array shows a maximum in the global entropy production, the Ge-Si-Ge array shows a minimum. For instance, in the interval from 40 to 60 nm the Si-Ge-Si array produces less entropy than the Ge-Si-Ge array. At the contrary, in 60-125 nm the Ge-Si-Ge array produces less than the Si-Ge-Si array. Finally, from 125 to 155 the situation inverts again. To close this discussion we remark the maximum in the global entropy production of the Ge-Si-Ge array around 145nm. This maximum is almost one order of magnitude bigger than any other maximum in the graph. The direction of laser incidence defines a kind of privileged direction in terms of the entropy generated in the system when there is not a symmetrical distribution of the materials in the system. Only one of the two possible incidence directions produces a minimum of entropy.

These results may be useful to the design of thin films used in electronic industry where the control of irreversible processes is an important issue.

Acknowledgements

FV acknowledges financial support by PROMEP and CONACYT (México) under contract 133763. JENC acknowledges financial support by CONACYT (México).

References

- Álvarez F.X., Jou D. (2007). Memory and nonlocal effects in heat transport: From diffusive to ballistic regimes. *Appl. Phys. Lett.*, 90, 083109.
- Figuroa A., Vázquez F. (2014). Optimal performance and entropy generation transition from micro to nanoscaled thermoelectric layers. *Int. J. Heat Mass Transf.*, 71, 724-731.

- Joshi A.A., Majumdar A. (1993). Transient ballistic and diffusive phonon heat transport in thin films. *J. Appl. Phys.*, 74, 31-39.
- Jou D., Casas-Vázquez J., Lebon G. (2001). “Extended Irreversible Thermodynamics 3rd edition” Springer.
- Lewandowska M., Malinowski L. (2006). An analytical solution of the hyperbolic heat conduction equation for the case of a finite medium symmetrically heated on both sides. *Int. Comm. Heat Mass Transf.*, 33, 61-69.
- Mansoor S.Bin, Yilbas B.S. (2011). Laser short-pulse heating of silicon-aluminum thin films. *Opt. Quant. Electron.*, 42, 601-618.
- Yilbas B.S., Al-Dweik A.Y. (2013). Short-pulse heating and analytical solution to non-equilibrium heating process. *Physica B*, 417, 28-32.